Available online at www.sciencedirect.com
SCIENCE DIRECT
ELSEVIER
Journal of the European Ceramic Society 26 (2006) 2685–2693
ECERS
www.elsevier.com/locate/jeurceramsoc

Glass-alumina functionally graded materials: their preparation and compositional profile evaluation

V. Cannillo, T. Manfredini, C. Siligardi *, A. Sola

Faculty of Engineering, Dipartimento di Ingegneria dei Materiali e dell'Ambiente University of Modena e Reggio Emilia, Via Vignolese 905, 41100 Modena, Italy

Received 26 January 2005; received in revised form 10 June 2005; accepted 18 June 2005
Available online 18 August 2005

Abstract

This work was focused on glass-alumina functionally graded materials (FGMs). For the glass phase, a proper composition was chosen belonging to the ternary system $CaO–ZrO_2–SiO_2$ and the substrate was made up of a sintered, high-purity polycrystalline alumina. Both of the ingredient materials were carefully characterized. The fabricated functionally graded materials were analysed in detail, by observing them under a scanning electron microscope (SEM) coupled with an X-ray energy dispersive spectrometer (X-EDS). The depth of penetration of the glass and the compositional profile were evaluated by means of a SEM-image elaboration. Moreover, this work applied an analytical model to predict the depth of penetration as a function of time and fabricating parameters such as temperature.

Keywords: Microstructure-final; $A1_2O_3$; Glass; FGM

1. Introduction

Functionally graded materials (FGMs) are a new class of composite materials, whose constituent phases are not evenly distributed in space, but give rise to a gradual change in composition and microstructure.[1]

In FGMs, the peculiar properties of the constituent phases can be fully exploited and, at the same time, abrupt bi-materials joints can be avoided. Mortensen and Suresh[2] underlined that in many applications thermo-mechanical loading conditions are different from point to point and therefore materials properties should vary with location as well. For example, the body of a gear should be tough but its surface should be hard and wear resistant. On the other hand, the direct coupling of heterogeneous materials often results in defects such as stress concentration, micro-cracking and delamination. Functionally graded materials can reduce such defects by making a gradual transition from one material to the other.[2]

Besides the continuity, a great advantage of functionally graded materials is their flexibility, since their properties can be optimised by properly choosing the ingredient materials nature, volume fraction and distribution.[3] In other words, the gradient in composition, microstructure and related properties can be tailored to the application, in order to achieve the best response to the specified service conditions. Cho and Ha,[4] for example, developed a numerical procedure, based on the finite difference method, in order to reduce steady-state thermal stresses in $Ni-Al_2O_3$ FGMs.

Sometimes functionally graded materials reach special performances, which differ from those of the constituent phases considered separately. Many researchers focused on FGMs peculiar properties. Among them, Jitcharoen et al. studied a glass-alumina functionally graded material, obtained by means of percolation of a $CaO–Al_2O_3–SiO_2$ molten glass into a polycrystalline alumina substrate. The gradual change of composition with depth gave rise to a smooth increase of the elastic modulus, which, in turn, improved the superficial hardness, enhanced the contact-damage resistance and substantially suppressed the formation of Hertzian cone cracks.[5] Moreover, they demonstrated

* Corresponding author. Tel.: +39 59 378416; fax: +39 59 373643.
E-mail address: siligardi@unimo.it (C. Siligardi).

0955-2219/$ – see front matter © 2005 Elsevier Ltd. All rights reserved.
doi:10.1016/j.jeurceramsoc.2005.06.046

that the controlled gradient in elastic modulus of the glass-alumina functionally graded material could result in an enhancement in the superficial resistance to frictional sliding contact.[6] Therefore, the overall behavior of such functionally graded materials differed relevantly from that of the alumina alone and also from that of a traditional glass-alumina composite material having the same mean composition.

Since FGMs offer several benefits, many specific fabrication techniques have been developed which can be roughly classified into two groups, i.e. constructive techniques and transport based techniques.[1,2] In the first group, the gradient is built layer by layer and therefore the resulting FGM is a multilayered system, made up of several strata, each of which has a mean composition slightly different from that of the neighbouring layers. The methods belonging to the second group are based on natural transport phenomena, such as the diffusion of atomic species, the conduction of heat or the flow of a liquid, in order to create a gradient in composition and/or microstructure. The aforementioned glass-alumina FGMs investigated by Jitcharoen et al., for examples, were produced thanks to a natural percolation process which occurs during a heat treatment.[5,6]

In the present work, the glass attitude to penetrate into a polycrystalline alumina substrate during a heat treatment was exploited to develop a new glass-alumina functionally graded material. The investigation was focused not only on the FGM fabrication and experimental characterization, but also on the prediction of the final depth of penetration of glass.

2. Experimental procedure

2.1. Ingredient materials characterization

2.1.1. Glass

As mentioned above, the glass used to fabricate the FGM samples belonged to the ternary system $CaO–ZrO_2–SiO_2$ (CZS) and its formulation, expressed in oxide molar percentages, is detailed in Table 1. The glass composition did not include any Al_2O_3, thus making easier the characterization of the final functionally graded materials. Moreover, the glasses belonging to the CZS system usually show not only interesting mechanical properties, such as a high Young's modulus and relatively good fracture toughness, but also remarkable chemical and physical characteristics.[7–9] Finally, the glass composition could be designed in order to achieve a coefficient of thermal expansion quite similar to that of the alumina.

In order to produce the glass, the powder raw materials (quartz, calcium carbonate and zirconium silicate) were mixed, dry ball milled for 30 min, decarbonated and melted in a platinum crucible at 1550 °C for 1 h. The glass was poured onto a graphite mould, thus obtaining a bar. In order to relax the thermal stresses, the glass body was annealed at 800 °C, just above the glass transition temperature, for 1 h. Finally, the glass bar was sliced, each slice being about 1 mm thick. Some glass specimens were specifically prepared for the glass characterization.

Table 1
Glass composition expressed in oxide molar percentage

	Glass composition (oxide)		
	CaO	ZrO_2	SiO_2
mol%	39.78	4.52	55.70

The glass thermal behaviour was evaluated by means of a differential thermal analysis (DTA), which was performed by heating 30 mg of glass powder from room temperature to 1400 °C at 10 °C/min (NETZSCH – DSC 404). A glass sample was observed under a heating microscope in order to gain a deeper insight into its thermal behaviour, which could significantly affect the FGM fabrication process. The coefficient of thermal expansion was quantified by heating a glass bar (45 mm × 5 mm × 5 mm) from room temperature up to the glass transition temperature at 20 °C/min (NETZSCH - DIL 404). The Young's modulus and the Poisson coefficient of the glass were measured by means of a resonance technique (EMOD, Lemmens Grindosonic® MK5) on a disk shaped (50 mm diameter) sample.

In order to analyse the hardness characteristics of the glass, a sample was embedded in unsaturated polyester resin and carefully polished, thus ensuring a perfectly planar surface. Then multiple Vickers micro-indentation tests were performed (Remet HX-1000 Microindenter), by applying a 25 g_f load for 15 s. For the sake of reliability, the micro-indentation test was repeated applying a 50 g_f load for the same time. At each load level, at least 20 measurements were made. The indented sample was observed under a SEM (Philips XL-40) and the permanent indent diagonals were measured. The Vickers hardness was deduced by the analysis of the permanent indents.[10] The same procedure was repeated applying a load of 100 g_f, which caused the glass to crack. Therefore, the permanent indents could be used to evaluate the glass fracture toughness (K_{IC}).[11]

2.1.2. Alumina

The FGM substrate was made up of a commercial alumina (mean grain size: 1 μm; purity: 99.9%, with minor traces of Fe_2O_3, SiO_2 and Na_2O[12]). Since the FGM fabricating process consisted in a heat treatment, the alumina mineralogical evolution as a function of temperature was investigated. An alumina sample underwent a X-ray diffraction, then the specimen was heat-treated following the same cycle used for the functionally graded materials (isothermal step lasting 4 h) and the X-ray analysis was repeated.

As already mentioned, the functionally graded materials were fabricated by means of percolation of glass into the substrate, therefore the alumina porosity was a really important parameter. The alumina porosity was indirectly deduced from the density measurement, which was carried out with a helium pycnometer (Micromeritics, AccuPyc 1330). Besides this, a more detailed analysis of the porosity could be developed by using the SEM micrographs of the alumina

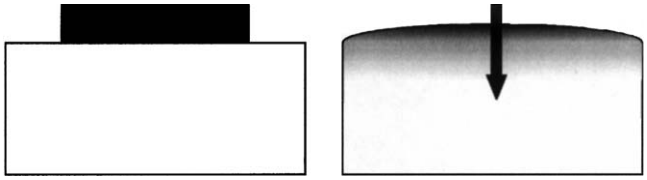

Fig. 1. Glass percolation into the polycrystalline alumina substrate induced by the heat treatment.

cross section, which were elaborated via an image analysis program.

The alumina thermo-mechanical properties (coefficient of thermal expansion, Young's modulus, Poisson coefficient) were measured in the same way as those of the glass. The Vickers microindentation test under a load of 500 g_f for 15 s allowed to evaluate the alumina hardness, while the permanent indents under a load of 1000 g_f for 15 s, which showed some cracks, were used to quantify the fracture toughness.

2.2. Functionally graded materials

Functionally graded materials were fabricated via percolation of the molten glass into the alumina substrate (Fig. 1). In order to fabricate a FGM specimen, a glass slice was placed onto an alumina bulk, as schematically shown in Fig. 1; since they were already flat, the glass and the alumina surfaces were not polished. Then the alumina and the glass were heat treated. Two different thermal treatments were tried out: both of them included heating from room temperature to 500 °C at 5 °C/min and then heating to 1600 °C at 10 °C/min; some samples were left at this temperature for 2 h, others for 4 h; finally, the systems were cooled down to 1000 °C at 20 °C/min. In both cases, during the heat treatment a second glass slice was placed on a platinum sheet next to the FGM sample and then it was analysed via X-ray diffraction. This procedure aimed at checking the glass behavior during the FGM heating cycle.

With the intent of testing the eventual crystallization of new phases in the functionally graded materials, an X-ray diffraction was performed on the cross section of the sample heat-treated at 1600 °C for 4 h.

The study of the effects induced by the glass penetration was carried out with a SEM coupled with a X-EDS. A special care was devoted to the FGM resulting microstructure and to the depth of penetration. A FGM sample, left at the maximum temperature for 4 h, was cut along the glass penetration direction and the cross section was carefully polished. Then the cross section was chemically etched with a 4% hydrofluoric acid (HF) for 10 s at room temperature. The selective etching removed the glass, leaving the alumina untouched. The domains occupied by the alumina and those previously occupied by the glass turned out to be clearly visible. While observing by SEM the etched FGM cross section, several, partially overlapped micrographs were taken along the depth and then joined (like a jigsaw puzzle) thus creating a picture of the full graded profile, up to the maximum depth of penetration reached by the glass, as shown in Fig. 2. In order to evaluate the compositional gradient, such column-like image was divided into 10 areas, in each of which the glass volume fraction was evaluated via an image analysis software.

3. Results

3.1. Ingredient materials

3.1.1. Glass

The trend of the DTA curve, Fig. 3, reveals that the glass transition occurs at about 790 °C. The evident exothermal peak at about 1000 °C may be due to the crystallization of wollastonite as main phase and a calcium–zirconium silicate, $Ca_2ZrSi_4O_{12}$, as secondary phase.[7,13] The spectrum also shows two endothermal peaks: the former, at about 1240 °C, is associated with the transformation of the wollastonite into pseudo-wollastonite; the latter, at about 1380 °C, may be caused by the complete softening of the glass or, most probably, by the melting of one of the crystal phases.[7,13] The study of the thermal behaviour also involves observation of the glass using a heating microscope. In this way, the sintering temperature can be located at 860 °C and the softening point at 950 °C. The identified characteristic temperatures of the glass phase are therefore: the glass transition temperature at 790 °C, the sintering temperature at 860 °C and the softening point at 950 °C. As already mentioned, the glass thermal reactivity during the actual FGM heat treatments was investigated by processing two glass slices together with the FGM samples. At the end of the two thermal cycles attempted, the glass slices appear completely transparent and the X-ray diffraction proves that no crystallization occurred.

The coefficient of thermal expansion, which should be comparable with that of the alumina, results to be $8.65 \times 10^{-6}\,K^{-1}$, as shown in Fig. 4.

The resonance-based measurements confirm that the chosen glass has good mechanical properties,[7] since the values of the Young's modulus and the Poisson coefficient are 96.18 GPa and 0.27, respectively. After performing the Vickers micro-indentations, the hardness could be calculated by measuring the indent size.[10] The Vickers hardness is therefore $Hv = 671 \pm 59\,kg/mm^2 = 6.58 \pm 0.58$ GPa. Since the Vickers indents under 100 g_f for 15 s were evidently cracked (Fig. 5), they could be used to evaluate the glass fracture toughness by applying the Evans and Charles equation[11]:

$$K_c = 0.1777 Hv \frac{a^2}{c^{3/2}} \quad (1)$$

where Hv is the Vickers hardness (in GPa), a is the length of the indent semi-diagonal (in μm) and c is the length of the crack path measured from the centre of the indent (in μm). It follows: $K_c = 0.86 \pm 0.13\,MPa\,m^{1/2}$. Both the Vickers hardness and fracture toughness are high in value for a glass, presumably because of the relevant percentage of ZrO_2 which is present in the glass formulation.

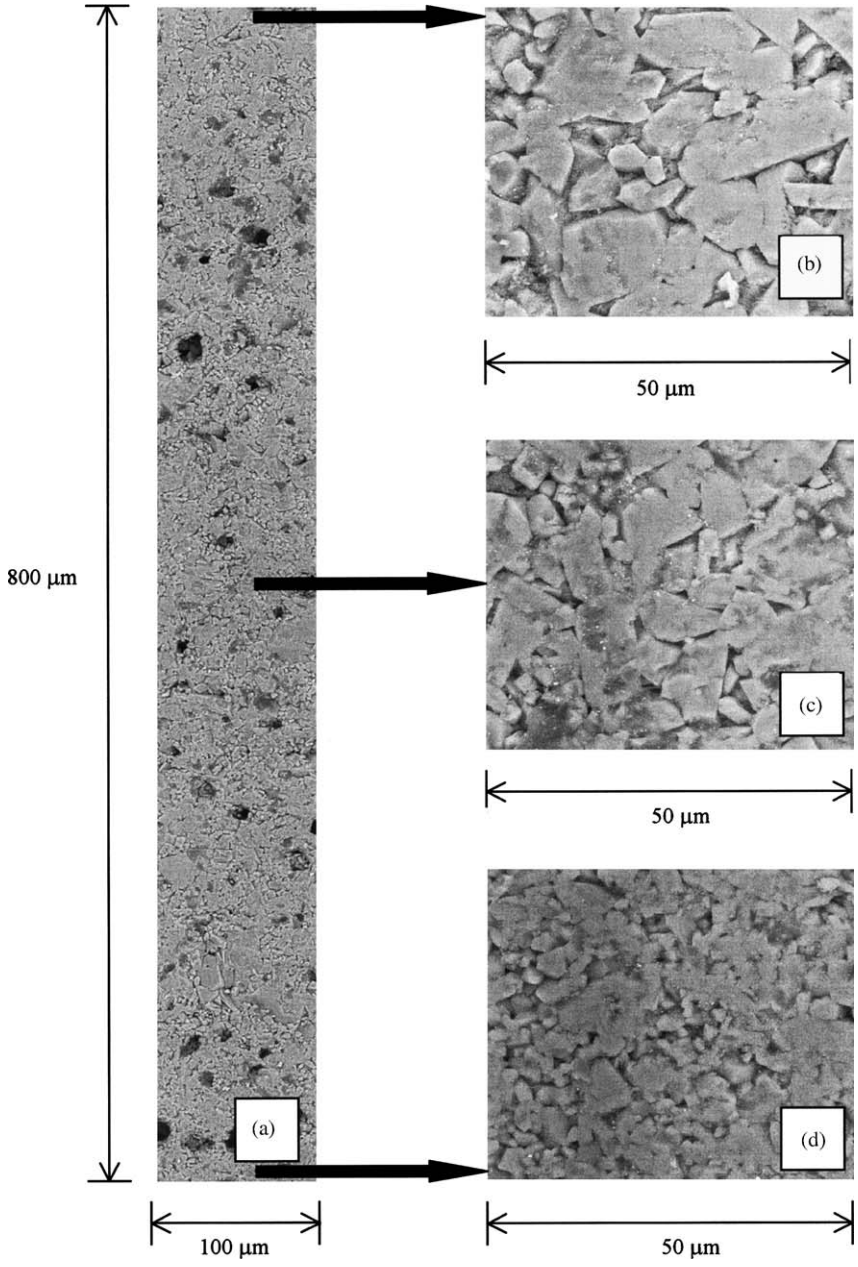

Fig. 2. Several SEM photographs were joined in order to obtain an image of the entire FGM cross section, up to the maximum depth reached by the glass (a). The details (b–d), which represent the FGM microstructure at 0 μm, 400 μm and 800 μm of depth, make more evident the microstructural gradient. The FGM microstructure was made more evident via a chemical etching, which removed the glass without modifying the alumina.

3.2. Alumina

On the basis of the X-ray diffraction (Philips PW 3710), the alumina is actually made up of only one crystal phase, since the diffraction peaks are all due to α-alumina (corundum syn.). On the basis of the XRD pattern, it is possible to exclude a relevant presence of amorphous phase in the alumina sample. The diffraction pattern of the heat-treated alumina specimen shows that no polymorphous transformation takes place, since the peaks are substantially the same. After the heat treatment, however, the peaks are narrower due to an increase in the alumina crystallite size, which could be evaluated by means of the Scherrer equation.[14,15] The comparison between the XRD patterns shows that the mean crystallite size increased about 18%. It is worth noting that the Scherrer equation applies to the size of crystallites, i.e. coherent domains of diffraction, which are sub-microscopic features. At the microscale, the alumina microstructural features were not significantly affected by the heat-treatment. Though a grain growth surely occurred, it is hard to quantify it, since the SEM observation enables to see aggregates of grains and not single grains (Fig. 6a and b).

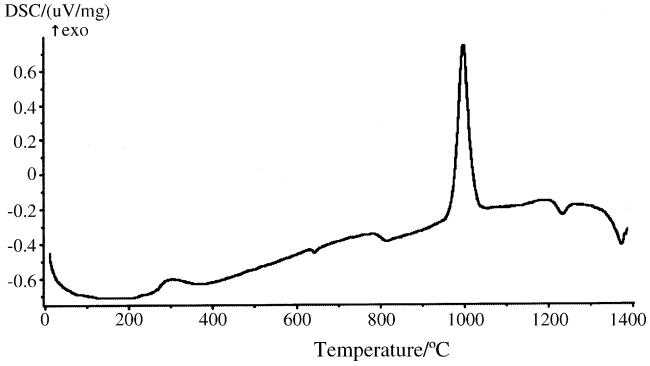

Fig. 3. The differential thermal analysis performed on the glass powder.

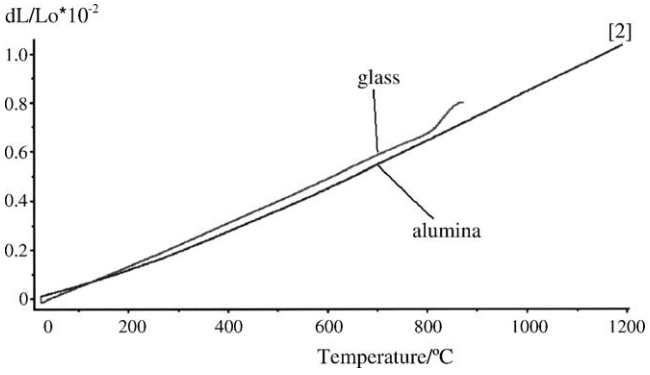

Fig. 4. The coefficients of thermal expansion of the FGM ingredient materials are really similar: $8.65 \times 10^{-6}\,K^{-1}$ for the glass and $8.18 \times 10^{-6}\,K^{-1}$ for the alumina.

Besides the mean grain size, a really important microstructural feature is the alumina porosity. Indeed a special attention should be paid to the measurement of the porosity and mean pore radius, since the glass mainly percolates along the alumina grain boundaries and fills the substrate pores.[16] These features were evaluated by following two alternative approaches. As a matter of fact, the porosity could be deduced from the apparent density value and it could be measured via a SEM image elaboration. The first method returned an apparent density of $3.819\,g/cm^3$, which was compared with the theoretical density of a full-sintered alumina,[17] i.e. $3.986\,g/cm^3$, in order to evaluate the residual porosity:

$$\frac{\rho_{fs} - \rho_m}{\rho_{fs}} \times 100 = \%\,\text{porosity} \quad (2)$$

where ρ_{fs} is the theoretical full-sintered density and ρ_m is the measured density. The total porosity results 4.2%. The SEM image elaboration returns a mean pore radius equal to $0.44 \pm 0.5\,\mu m$ and a related mean porosity of $4.6 \pm 0.6\%$, which is in really good agreement with the aforementioned value.

As concerns the alumina thermo-mechanical characteristics, the coefficient of thermal expansion results to be $8.18 \times 10^{-6}\,K^{-1}$ (Fig. 4). Therefore, the coefficients of thermal expansion of the FGM ingredient materials are quite similar, thus significantly reducing the residual ther-

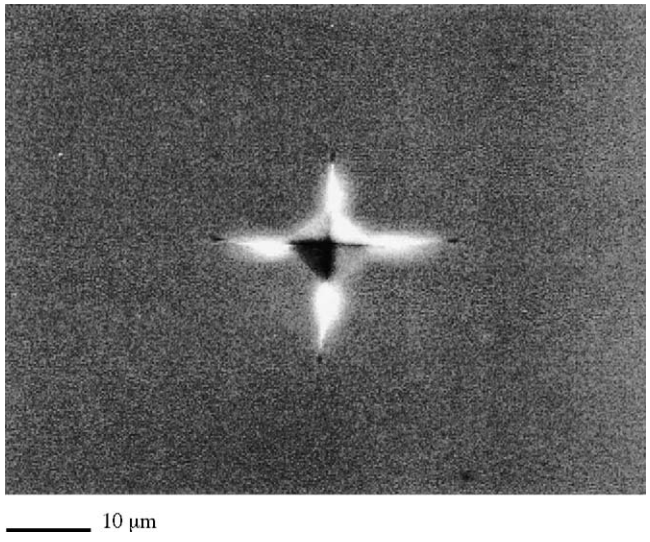

Fig. 5. Typical glass micro-indentation under a load of $100\,g_f$ applied for 15 s.

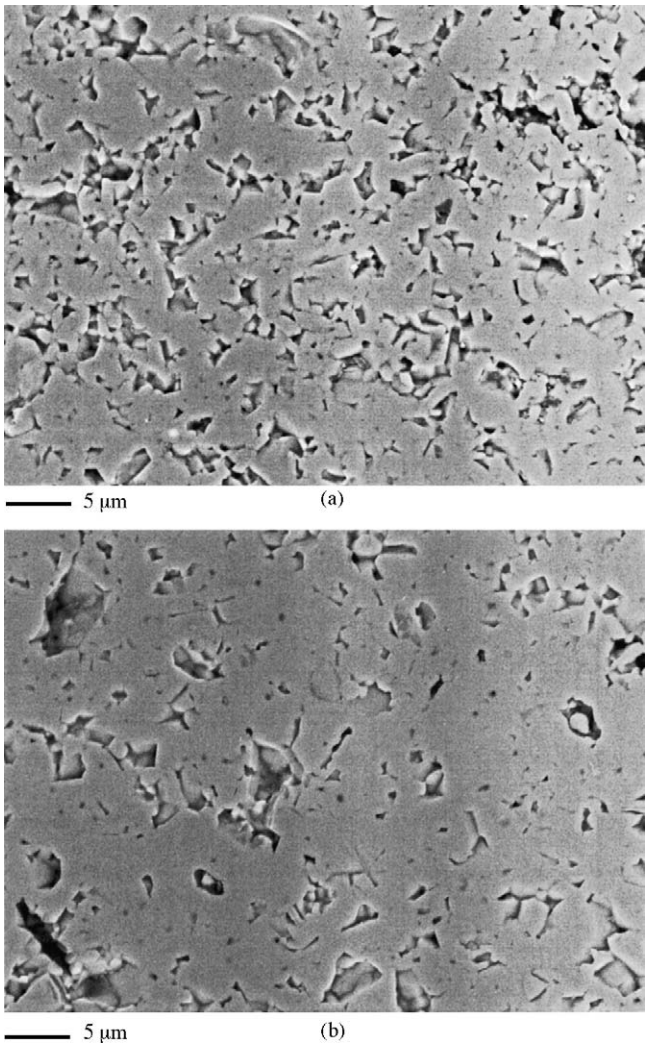

Fig. 6. The alumina cross section was observed by using a scanning electron microscope before (a) and after the heat treatment (b).

Table 2
Thermo-mechanical properties of the ingredient materials

	Glass	$A1_2O_3$
Young's modulus (GPa)	96.18	358.3
Poisson coefficient	0.27	0.2
Coefficient of thermal expansion (K^{-1})	8.65×10^{-6}	8.18×10^{-6}
Vickers hardness (GPa)	6.58	15.41
Toughness (MPa $m^{1/2}$)	0.86	2.6

mal stresses which may arise during the FGM fabrication process. Finally, the alumina Young's modulus and Poisson coefficient, measured by means of the resonance technique, are 358.3 GPa and 0.2, respectively. The permanent indents under a load of 500 g_f applied for 15 s. were measured and the Vickers hardness was calculated[10] to be $Hv = 1571 \pm 144\ kg/mm^2 = 15.41 \pm 0.41$ GPa. The fracture toughness evaluation gives a value consistent with that supplied by the manufacturer, that is to say 2.6 MPa $m^{1/2}$.[12] The properties of the FGM constituent phases are briefly listed in Table 2.

3.3. Functionally graded materials

The diffraction pattern of the FGM cross section is substantially analogous to that of the alumina alone, since all the peaks can be attributed to the α-alumina. This means that neither the heat treatment nor the glass penetration give rise to the crystallization of new phases.

Independently of the heat-treatment performed during fabrication, the SEM observation confirms that the glass penetrates into the alumina moving along its grain boundaries and partially filling the alumina pores. In fact, as already observed by Cannillo et al.[18] the resulting FGM microstructure is formed by finite and distinguished domains – the alumina grains and the glass areas at the grain boundaries and pores. However, the glass volume fraction progressively diminishes along the penetration direction, thus creating the overall compositional and microstructural profile. Though the glass filled the alumina pores, some residual pores can be observed.

As for the X-EDS analysis, the molar percentages of Al_2O_3 and SiO_2 were measured as a function of depth (Fig. 7a and b). As a matter of fact, the SiO_2 can be assumed as a marker of the glass and the absence of Al_2O_3 from the glass composition makes simpler the distinction between the two ingredient materials. The SiO_2 molar percentage goes to zero at 460 μm in the sample heat-treated at 1600 °C for 2 h and at about 800 μm in the sample heat-treated at 1600 °C for 4 h; these values can be considered as the depths reached by the glass. The experimental compositional profiles do not follow a strictly monotonic trend; in the graph referring to the specimen heat treated for 2 h, for example, the SiO_2 percentage approaches 0 at around 300 μm, then slightly increases again and finally becomes 0 at 460 μm. This is due to the fact that the X-EDS chemical analysis is performed on single points, whilst the FGM microstructure is discrete, as mentioned above.

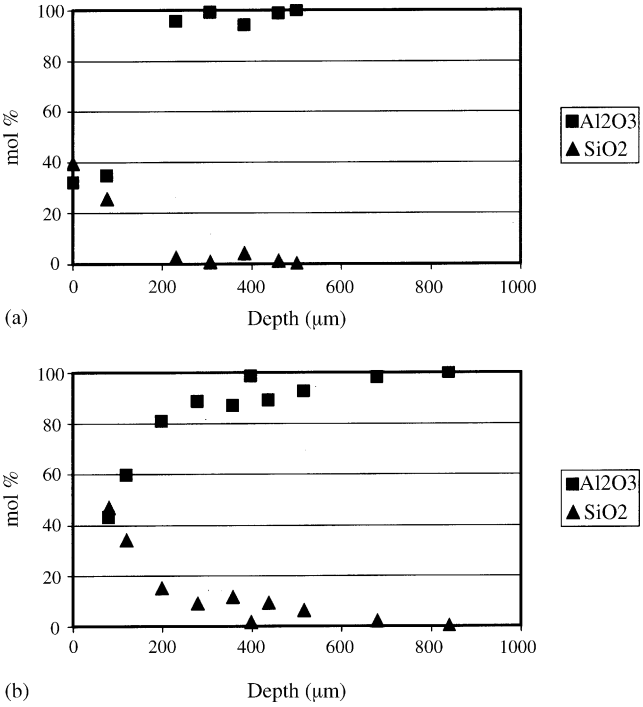

Fig. 7. The X-EDS profiles do not follow a monotonic trend. However, they are useful in order to define the depth of penetration reached by the glass, which is about 460 μm for the FGM samples treated at 1600 °C for 2 h (a) and about 800 μm for the samples left at 1600 °C for 4 h (b).

For the FGM system left at 1600 °C for 4 h, a more reliable description of the compositional profile was obtained via an image elaboration of the chemically etched cross section. Since the acid corrosion removes the glass, the microstructural details are highlighted and it is possible to distinguish the alumina grains from the domains previously occupied by the glass. Via an image elaboration the glass volume fraction can be measured as a function of depth, assuming that the glass volume is equivalent to the volume remained empty after the chemical etching (Fig. 8). A parabolic trend could be defined with a least square approximation method:

$$y = -0.00005x^2 + 0.00730x + 22.366$$

where y is the volume fraction and x is the depth (Fig. 9).

4. Analytical modelling

Since the functionally graded material behaviour is deeply influenced by the compositional and microstructural gradient and by the degree of penetration,[5,19] it would be desirable to predict the depth of penetration of glass induced by a specified fabricating process.

By assuming that the driving force for percolation is capillarity, Kuromitsu et al.[19] proposed a penetration model which relates the depth of penetration to time by means of a coefficient which, in turn, depends on material properties at a fixed

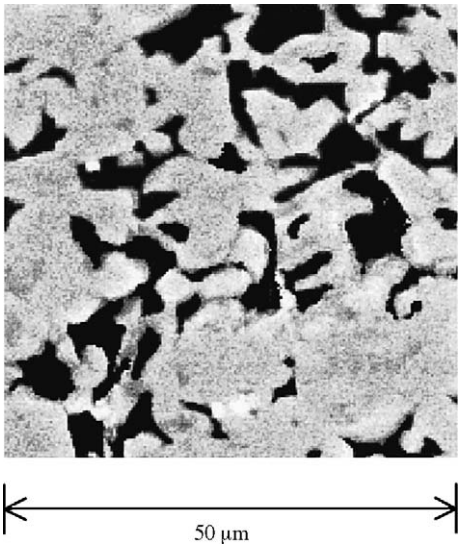

Fig. 8. The column-like image of the graded profile after the chemical etching was elaborated in order to mark the areas originally occupied by the glass (in black); the example represented here refers to the analysis of an area at about 20 μm of depth.

temperature[19]:

$$L = Kt^{1/2} \tag{3}$$

where L is the glass penetration depth, t is time and K, usually defined as the coefficient of penetration, is expressed by the relation[19]

$$K = \sqrt{\frac{r\cos\theta}{2}\frac{\gamma}{\eta}} \tag{4}$$

where r is the capillary radius, θ is the contact angle, y the surface tension of glass and η is its viscosity, referred to the fabricating temperature (e.g. 1600 °C).

The capillary radius (r) could be assimilated to the mean pore radius of the alumina substrate, which was measured to be 0.44 μm.

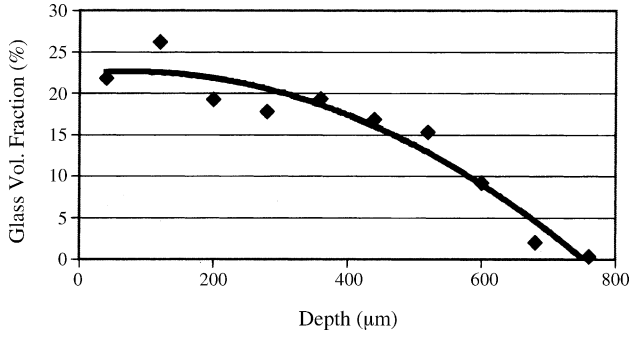

Fig. 9. The graphic represents the glass fraction as a function of depth. The full profile SEM picture was divided into 10 fields, each field being 80 μm deep and 100 μm wide. Afterward the glass fraction was measured in each field via an image analysis software. With a least square approximation, a parabolic trend could be defined.

The contact angle (θ) could be assumed to be 0, since the wettability between the molten glass and the alumina is good,[19] as it may by deduced be the FGM superficial state.

The glass surface tension (γ) was estimated by applying the Appen equation, which is based on the hypothesis that the surface tension is an addictive property, whose value can be expressed as a linear function of the oxide molar percentages. The surface tension was therefore calculated according to the equation[20]:

$$\gamma = \frac{0.510m_c + 0.350m_z + 0.290m_s}{100} \tag{5}$$

where m_c, m_z and m_s (Table 1) are the molar percentages of CaO, ZrO_2 and SiO_2, respectively. It is worth noting, however, that the Appen equation applies at 1300 °C instead of 1600 °C, which is the fabricating temperature. Since the glass composition does not contain any B_2O_3, it is reasonable that the glass surface tension decreases gradually if the temperature rises from 1300 °C to 1600 °C.[20] To sum up, the glass surface tension at 1600 °C could be assumed to be 0.365 N m^{-1}.

The glass viscosity was calculated by means of the Vogel, Fulcher and Tamman equation[20]:

$$\log\eta = A + \frac{B}{T - T_0} \tag{6}$$

where A, B, T_0 are three coefficients, T is the temperature (in K) and η is the viscosity. The constants could be determined on the basis of the glass characteristic temperatures and related viscosities: at the glass transition temperature (790 °C) the viscosity is $10^{13.3}$ dPa s, at the sintering temperature (860 °C) it is $10^{9.0}$ dPa s and at the softening point (950 °C) it is $10^{6.6}$ dPa s.[21] The viscosity was therefore $10^{3.30}$ dPa s at 1600 °C.

By substituting in Eq. (4), the coefficient of penetration, K, at 1600 °C resulted to be 0.0642×10^{-4} m/s$^{1/2}$. Finally, the depth of penetration after 2 h and 4 h turned out to be 544 μm and 800 μm, respectively.

5. Discussion

The production of a functionally graded materials breaks down into two main steps: first of all, the compositional and microstructural profile should be optimised in function of the materials properties required by the specified application; then the designed gradient should be realized in a controlled and reproducible way. This target can be achieved by means of an appropriate fabrication technique.[22]

Glass-alumina functionally graded materials can be easily fabricated by means of percolation of molten glass into a polycrystalline bulk alumina. The basic idea of the production technique, which exploits a natural transport phenomenon,[2] is easy. However, an accurate investigation of the resulting graded profile is required.

A detailed characterization of the FGM constituent phases is required, as the properties of glass and alumina may significantly influence the fabricating process and the FGM overall behavior. Since functionally graded materials are fabricated via a thermal treatment, the glass and alumina thermal behavior was accurately investigated. As for the glass, the differential thermal analysis suggests that some wollastonite and calcium–zirconium silicate crystallize at 1000 °C and then some wollastonite turns into pseudo-wollastonite at 1240 °C. Nevertheless, the reference glass samples, heat treated by applying the FGM fabrication cycle, remain perfectly amorphous. The non-crystallization of the glass is likely to be due to the applied thermal cycle, which is not favourable to the nucleation of new crystal phases such as the wollastonite. As a matter of fact, when the FGM specimens are produced, the glass completely melts during the isothermal step, then it is quickly cooled down to 1000 °C and abruptly extracted from the furnace. As a consequence, the crystallization phenomena, which are located at about 1000 °C, have no time to occur. Moreover, it should be remarked that the DTA was performed on a small quantity of glass powder, while the FGM production required a glass bulk; therefore, the crystallization kinetics could be significantly different. As far as the alumina is concerned, the diffraction analysis, performed before and after the thermal treatment, proves that the alumina is thermally stable, as no polymorphous transformation took place. Yet, the pattern peaks are narrower as a consequence of the alumina grain growth. It would be interesting, as a future development of this research, to evaluate more carefully the effects of the alumina grain growth, which could be associated with other microstructural changes such as a porosity evolution.

As regards the X-ray diffraction of the functionally graded materials, the patterns confirm that the glass penetration and the heat treatment do not induce a significant development of new crystal phases. On the other hand, the EDS chemical analysis suggests that the FGM microstructure consists of distinct domains of glass and alumina, thus proving the microstructural heterogeneity of the system. The XRD and the SEM inspection suggest that the FGM production did not induce a relevant appearance of new crystal phases. However, it is not possible to exclude that an interdiffusion locally occurred at the nanoscale at the glass-alumina interface.

One more problem connected with the described fabricating process is represented by the arising of thermal residual stresses. Indeed, functionally graded materials are multiphase systems and the mismatch in thermo-mechanical properties could result in thermal residual stresses, due to the differential contraction during the final cooling down step. Dao et al. developed a micromechanical computational method in order to investigate the combined effects of microstructural heterogeneity and thermo-mechanical properties mismatch. They demonstrated that high thermal residual stress concentrations could be predicted at the grain size level. These locally concentrated stresses, in turn, may trigger small cracks and voids, which sap the overall system resistance.[23] The choice of a proper glass composition may be beneficial to the FGM performances, by reducing the discrepancies between the thermo-mechanical properties of the constituent phases. The glass formulation which was used, belonging to the $CaO–ZrO_2–SiO_2$ system, fully satisfies this requirement since the glass shows favourable mechanical properties (Table 2) and, most of all, its coefficient of thermal expansion is quite similar to that of the substrate (Fig. 4). The minimized difference between the coefficients of thermal expansion of the constituent phases should significantly reduce the thermal residual stresses.

In view of a systematic application of the percolation technique, it would be desirable to define a correlation between the length of the thermal treatment and the depth of penetration. This result can be achieved by measuring the depth reached by the glass in specimens heat-treated for different times. The X-EDS profiles of the FGM cross sections are useful in order to estimate the depth reached by the glass, since they are able to detect the presence of the Silicon, which is a marker of the glass. The profiles do not follow a monotonic trend, because the FGM microstructure is discrete and random and the measurement is performed on single points. Nevertheless, a general trend can be defined and the depth of penetration can be deduced by the point where the Si percentage becomes zero. Alternatively, the FGM compositional gradient can be evaluated by means of the SEM image analysis. The accurate inspection of the specimen microstructure immediately reveals the depth reached by the glass. Furthermore, this approach allows to gain a deeper insight into the gradient profile. As a matter of fact, the full-profile image can be divided into a reasonable number of fields and the mean glass area fraction, which is representative of the volume fraction, can be evaluated in such fields. Since the proportions of the constituent phases are measured on fields and not on individual points, it is possible to define a smoother and more reliable compositional trend.

In this work, a different approach was adopted, which allows to predict the depth of penetration instead of measuring it a posteriori. Indeed, by assuming that the driving force for penetration is capillarity, it is possible to use an analytical model in order to predict the depth of penetration as a function of time and fabricating parameters (such as temperature).[19] The basic hypothesis that the infiltration is caused by capillarity is verified, since the FGM characterization proves that the glass penetrates into the alumina body by percolating along the grain boundaries. The predicted values and the experimental ones are in fairly good agreement, especially when the longer heating cycle is considered (Table 3). The discrepancies may be ascribed to the assumptions required to evaluate the glass properties at the fabricating temperature. In particular, the glass viscosity at 1600 °C was extrapolated by applying the Vogel–Fulcher–Tamman equation, but the equation constants were calculated on the basis of three characteristic temperatures which are much lower than the fabricating temperature. It follows that the prediction of viscosity

Table 3
Comparison between the experimental and calculated depths of penetration

	Time	
	2 h	4 h
Depth of penetration		
Experimental	460	800
Calculated	544	770

at high temperature could be inexact, thus slightly overestimating the real value. Moreover, when substituting in Eq. (3), the length of the only isothermal step was considered, but the heat treatment is longer and more complex. This remark justifies the fact that the difference between the predicted and the measured depths is greater when the shorter fabricating process is concerned. Finally, the FGM fabricating heat treatment was likely to induce a microstructural modification of the alumina substrate. The alumina grain growth, which was quantified via diffraction analysis, was presumably associated with an enhancement of the grain boundary morphology and a reduction of the mean porosity. These modifications might affect the prediction of the depth of penetration since they influence the mean pore radius. In spite of these limits, the penetration model described represents an efficient and reliable tool in order to estimate the depth reached by the glass.

6. Conclusions

Functionally graded materials are a new and appealing class of composite materials, whose peculiarity lies on the gradual change in composition, microstructure and related properties. In order to exploit the FGM benefits, however, the gradient should be properly designed and tailored to the application; moreover the fabricating process should be reliable and reproducible. Percolation of a molten glass into a polycrystalline alumina results a simple way to produce a Functionally graded material and the choice of a proper glass composition ensures the reliability of the process. Moreover, the depth of penetration, which is a key-factor of the realized gradient, can be predicted on the basis of the ingredient materials properties and fabrication parameters. Future developments will aim to develop a computational model suitable to predict the FGM elastic modulus gradient and thermal stresses.

References

1. Miyamoto, Y., Kaysser, W. A., Rabin, B. H., Kawasaki, A. and Ford, R. G., *Functionally Graded Materials Design, Processing and Applications*. Kluwer Academic Publishers, 1999.
2. Mortensen, A. and Suresh, S., Functionally graded metals and metal-ceramic composites. I. Processing. *Int. Mater. Rev.*, 1995, **40**(6), 239–265.
3. Cho, J. R. and Park, H. J., High strength FGM cutting tools: finite element analysis on thermoelastic characteristics. *J. Mater. Process. Technol.*, 2002, **130–131**, 351–356.
4. Cho, J. R. and Ha, D. Y., Optimal tailoring of 2D volume-fraction distributions for heat-resisting functionally graded materials using FDM. *Comput. Method Appl. Mech. Eng.*, 2002, **191**, 3195–3211.
5. Jitcharoen, J., Padture, N. P., Giannakopoulos, A. E. and Suresh, S., Hertzian-crack suppression in ceramics with elastic-modulus-graded surfaces. *J. Am. Ceram. Soc.*, 1998, **81**(9), 2301–2308.
6. Suresh, S., Olsson, M., Giannakopoulos, A. E., Padture, N. P. and Jitcharoen, J., Engineering the resistance to sliding-contact damage through controlled gradients in elastic properties at contact surfaces. *Acta Materialia*, 1999, **47**(14), 3915–3926.
7. Leonelli, C. and Siligardi, C., $CaO–SiO_2–ZrO_2$ glasses: modelling and experimental approach. *Recent Res. Dev. Mater. Sci.*, 2002, **3**, 599–618.
8. Cannillo, V., Manfredini, T., Montorsi, M., Siligardi, C. and Sola, A., Experimental characterization and computational simulation of glass-alumina functionally graded surfaces. *Materials Science Forum*, 2005, **492–493**, 647–652.
9. Cannillo, V., Manfredini, T., Siligardi, C. and Sola, A., Preparation and experimental characterization of glass-alumina functionally graded materials. *J. Eur. Ceram. Soc*., in press.
10. Quinn, G. D., Patel, P. J. and Lloyd, I., Effect of loading rate upon conventional ceramic microindentation hardness. *J. Res. Nat. Inst. Standards Technol.*, 2002, **107**(3), 299–306.
11. Ponton, C. B. and Rawlings, R. D., Vickers indentation fracture test. Part 1. Review of literature formulation of standardised indentation toughness equations. *Mater. Sci. Technol.*, 1989, **5**, 865–871.
12. FN S.p.A. Nuove tecnologie e Servizi Avanzati. Bosco Marengo (AL) Italy.
13. Siligardi, C., D'Arrigo, M. C., Leonelli, C. and Pellacani, G. C., Bulk crystallization of glasses belonging to the calcia–zirconia–silica system by microwave energy. *J. Am. Ceram. Soc.*, 2000, **83**(4), 1001–1003.
14. Cullty, D.B., *Elements of X-Ray Diffraction* (*2nd ed.*). Addison-Wesley Publishing Company, Inc.; Reading, MA, Menlo Park, California, London, Amsterdam, Don Mills, Ontario, Sidney, 1978.
15. Warren, B. E., *X-Ray Diffraction*. Dover Publications, 1996.
16. Flaitz, P. L. and Pask, J. A., Penetration of polycristalline alumina by glass at high temperatures. *J. Am. Ceram. Soc.*, 1987, **70**(7), 449–455.
17. Fang, T.-T., Shiue, J.-T. and Shiau, F.-S., On the evaluation of the activation energy of sintering. *Mater. Chem. Phys.*, 2003, **80**(1), 108–113.
18. Cannillo, V., Manfredini, T., Corradi, A. and Carter, W. C., Numerical models of the effect of heterogeneity on the behavior of graded materials. *Key Eng. Mater.*, 2002, **206–213**, 2163–2166 (Trans Tech Publications, Switzerland).
19. Kuromitsu, Y., Yoshida, H., Takebe, H. and Morinaga, K., Interaction between alumina and binary glasses. *J. Am. Ceram. Soc.*, 1997, **80**(6), 1583–1587.
20. Navarro, J. M. F., *El Vidrio*. C.S.I.C, Madrid, 1991.
21. Pascual, M. J., Pascual, L. and Duràn, A., Determination of the viscosity-temperature curve for glasses on the basis of fixed viscosity points determined by hot stage microscopy. *Phys. Chem. Glasses*, 2001, **42**(1), 61–66.
22. Kawasaki, A. and Watanabe, R., Concept and P/M fabrication of functionally graded materials. *Ceram. Int.*, 1997, **23**, 73–83.
23. Dao, M., Gu, P., Maewal, A. and Asaro, R. J., A micromechanical study of residual stresses in functionally graded materials. *Acta materialia*, 1997, **45**(8), 3265–3276.